

Superconductivity in $(\text{NH}_3)_y\text{Cs}_{0.4}\text{FeSe}$

Lu Zheng,¹ Masanari Izumi,¹ Yusuke Sakai,¹ Ritsuko Eguchi,¹ Hidenori Goto,^{1,2} Yasuhiro Takabayashi,¹ Takashi Kambe,³ Taiki Onji,³ Shingo Araki,³ Tatsuo C. Kobayashi,³ Jungeun Kim,⁴ Akihiko Fujiwara,⁴ and Yoshihiro Kubozono^{1,2,*}

¹Research Laboratory for Surface Science, Okayama University, Okayama 700-8530, Japan

²Research Center of New Functional Materials for Energy Production, Storage and Transport, Okayama University, Okayama 700-8530, Japan

³Department of Physics, Okayama University, Okayama 700-8530, Japan

⁴Japan Synchrotron Radiation Research Institute, RIKEN SPring-8 Center, Hyogo 679-5198, Japan

(Received 9 August 2013; revised manuscript received 11 September 2013; published 30 September 2013)

Alkali-metal-intercalated FeSe materials, $(\text{NH}_3)_yM_{0.4}\text{FeSe}$ (M : K, Rb, and Cs), have been synthesized using the liquid NH_3 technique. $(\text{NH}_3)_y\text{Cs}_{0.4}\text{FeSe}$ shows a superconducting transition temperature (T_c) as high as 31.2 K, which is higher by 3.8 K than the T_c of nonammoniated $\text{Cs}_{0.4}\text{FeSe}$. The T_c s of $(\text{NH}_3)_y\text{K}_{0.4}\text{FeSe}$ and $(\text{NH}_3)_y\text{Rb}_{0.4}\text{FeSe}$ are almost the same as those of nonammoniated $\text{K}_{0.4}\text{FeSe}$ and $\text{Rb}_{0.4}\text{FeSe}$. The T_c of $(\text{NH}_3)_y\text{Cs}_{0.4}\text{FeSe}$ shows a negative pressure dependence. A clear correlation between T_c and lattice constant c is found for ammoniated metal-intercalated FeSe materials, suggesting a correlation between Fermi-surface nesting and superconductivity.

DOI: 10.1103/PhysRevB.88.094521

PACS number(s): 74.70.Xa

Metal-intercalated FeSe superconductors are one of the most promising materials for high superconducting transition temperature (T_c), since an onset T_c (T_c^{onset}) as high as ~ 30 K was recently discovered in K_xFeSe and $\text{Cs}_{0.4}\text{FeSe}$.^{1,2} Many metal-intercalated FeSe materials have recently been synthesized by dissolving metals (Li, Na, K, Ca, Sr, Ba, Eu, and Yb) in liquid NH_3 containing β -FeSe, which intercalates the metal atoms into the FeSe crystals. The $\text{Na}_{0.5}\text{FeSe}$ sample prepared using the liquid NH_3 described above showed a very high T_c^{onset} (46 K).³ These materials must contain NH_3 between the FeSe layers, because their lattice constant c is expanded by at least 2.1 Å.^{1,3}

Thus, diverse metal-intercalated FeSe materials have been synthesized using liquid NH_3 . The structure of metal-intercalated FeSe containing NH_3 was clarified by Rietveld refinement of the neutron powder diffraction pattern of $\text{Li}_{0.6(1)}(\text{ND}_2)_{0.2(1)}(\text{ND}_3)_{0.8(1)}\text{Fe}_2\text{Se}_2$,⁴ showing the ND_3 to be surrounded by Li atoms to form the planar layer. This report demonstrates that a precise amount of NH_3 is incorporated in metal-intercalated FeSe containing NH_3 .⁴ Recently, two phases of $(\text{NH}_3)_y\text{K}_x\text{FeSe}$ were systematically investigated:⁵ $(\text{NH}_3)_{0.235}\text{K}_{0.15}\text{FeSe}$ with $T_c^{\text{onset}} = 44$ K and $(\text{NH}_3)_{0.185}\text{K}_{0.3}\text{FeSe}$ with $T_c^{\text{onset}} = 30$ K. These two phases are isostructural, but the c (15.56 Å) of the former phase is larger than the c (14.84 Å) of the latter. The c of 14.84 Å in the latter structure is still larger than that [$c = 14.0367(6)$ Å] in nonammoniated $\text{K}_{0.5}\text{FeSe}$ (T_c^{onset} of ~ 30 K).

In this paper, we report on the syntheses and physical properties of $(\text{NH}_3)_yM_x\text{FeSe}$ (M : K, Rb and Cs), which were prepared using liquid NH_3 . The synthesis of these materials is important because of a lack of systematic studies on superconductivity in alkali-metal-intercalated FeSe. When the T_c s obtained in this and earlier studies³⁻⁵ are plotted as a function of ionic radius and the lattice constant c , a clear correlation between T_c and c can be seen. Such plots are important to clarify a key parameter in this class of superconductors. Furthermore, we report on the pressure dependence of T_c in $(\text{NH}_3)_y\text{Cs}_{0.4}\text{FeSe}$ and on pressure effect on superconductivity in $(\text{NH}_3)_yM_x\text{FeSe}$. The study of pressure

effect is important to establish the correlation between T_c and c , i.e., to pursue whether the lattice constant c is a universal scaling factor for explaining the superconductivity.

The β -FeSe sample was prepared with the annealing method; details are described in the supplemental material.⁶ The x-ray diffraction and magnetic susceptibility, M/H , of the prepared β -FeSe were measured and compared with previous reports⁷ to confirm the sample quality; M and H correspond to magnetization and applied magnetic field, respectively. The samples of $(\text{NH}_3)_yM_x\text{FeSe}$ were prepared by the liquid NH_3 technique; details are described in the Supplemental Material.⁶

The x-ray diffraction and M/H of the $(\text{NH}_3)_yM_x\text{FeSe}$ samples were measured with synchrotron radiation [$\lambda = 0.40045(1)$ Å] at BL02B2 of the Super Photon ring-8 (SPring-8) and a superconducting quantum interference device (SQUID) magnetometer (Quantum Design MPMS2), respectively. The unit-cell parameters were determined by Rietveld refinement,⁸ crystallographic data, including atomic coordinates and fraction of phases, are listed in the Supplemental Material.⁶ The resistance R of the samples was recorded in standard four-terminal measurement mode with a He-flow cryostat regulated by a temperature controller (Oxford Instrument ITC503). The electric current I was supplied by a Keithley 220 programmable current source, and the voltage was measured by a Keithley nanovoltmeter 2182. The real part χ' of the alternating current (ac) magnetic susceptibility⁹ and the M/H under high pressure were measured using the Hartshorn bridge method⁹ and the above SQUID magnetometer, respectively. For high-pressure ac susceptibility measurement, the sample was introduced into an indenter cell, while the sample was introduced into a piston-cylinder-type BeCu cell for high-pressure M/H measurement with the SQUID. All measurements were performed without any exposure of the samples to air. Throughout this paper, chemical formulas are written using the experimental nominal values.

Figure 1(a) shows the x-ray diffraction pattern of the prepared FeSe sample. The pattern was analyzed by Rietveld refinement with the crystal structure (tetragonal crystal and space group $P4/nmm$) reported previously.⁷ The lattice

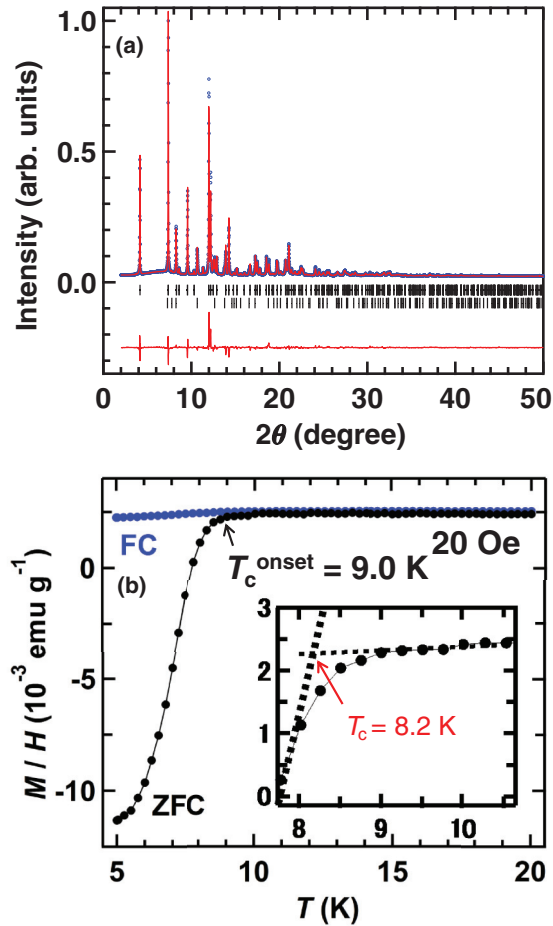


FIG. 1. (Color online) (a) X-ray diffraction pattern and (b) M/H - T plots of the FeSe sample. In (a), the experimental x-ray diffraction pattern (blue circles) can be reproduced by the pattern (red line) calculated from the two phases β -FeSe (80%) and α -FeSe (20%); the black ticks show the 2θ positions predicted for β -FeSe (top) and α -FeSe (bottom). The lower red line shows the difference between experimental and calculated patterns.

constants were determined to be $a = 3.77179(4)$ and $c = 5.5234(1)$ Å, which are almost the same as those reported previously [$a = 3.7747(1)$ and $c = 5.5229(1)$ Å].⁷ From the analysis, it has been suggested that an $\sim 20\%$ fraction of non-superconducting α -FeSe is present, with 80% superconducting β -FeSe, in the sample; the crystallographic data are shown in the Supplemental Material.⁶ The M/H is recorded as a function of temperature T [Fig. 1(b)] in zero-field cooling (ZFC) and field cooling (FC). The M/H clearly drops below 9 K ($T_c^{\text{onset}} = 9.0$ K, $T_c = 8.2$ K). The T_c^{onset} and T_c are the same as those of β -FeSe reported previously.⁷ The shielding fraction was evaluated to be 92% at 5 K from the M/H - T plot in ZFC mode, substantially consistent with the fraction ($\sim 80\%$) of β -FeSe determined from x-ray diffraction.

Figure 2(a) shows the x-ray diffraction pattern of $(\text{NH}_3)_y\text{Cs}_{0.4}\text{FeSe}$. The x-ray diffraction peaks were analyzed by Rietveld refinement with the space group of $I4/mmm$ (body-centered tetragonal crystal lattice) in the same manner as nonammoniated $\text{K}_{0.5}\text{FeSe}$, which was prepared by the annealing method.¹ The crystal structure of $(\text{NH}_3)_y\text{Na}_{0.5}\text{FeSe}$ was analyzed with the same space group.³ The lattice constants

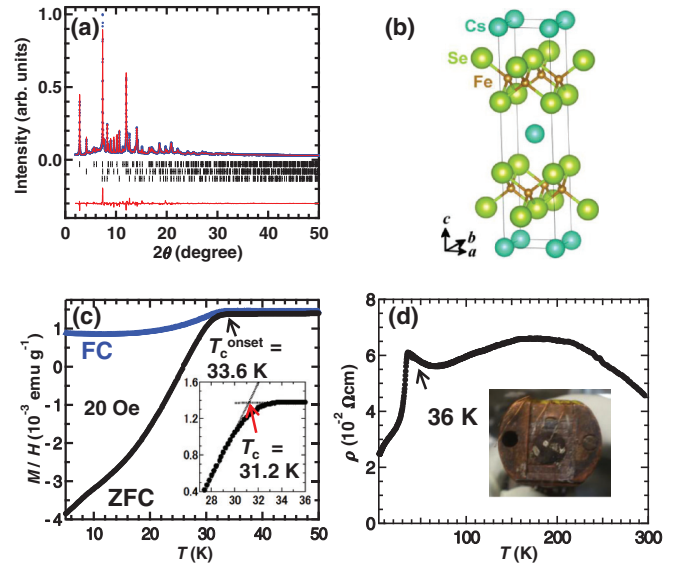


FIG. 2. (Color online) (a) X-ray diffraction pattern, (b) schematic crystal structure, (c) M/H - T plots, and (d) ρ - T plot of the $(\text{NH}_3)_y\text{Cs}_{0.4}\text{FeSe}$ sample. In (a), the experimental x-ray diffraction pattern (blue circles) can be reproduced by the pattern (red line) calculated from the three phases $(\text{NH}_3)_y\text{Cs}_{0.255(5)}\text{FeSe}$ (37%), β -FeSe (37%), and α -FeSe (26%); the black ticks show the 2θ positions predicted for $(\text{NH}_3)_y\text{Cs}_{0.255(5)}\text{FeSe}$ (top), β -FeSe (middle), and α -FeSe (bottom). The lower red line shows the difference between experimental and calculated patterns. In (b), NH_3 molecules are not shown. In (d), a picture of the pellet used for ρ measurements is inset. Its L , W , and d were 0.108, 0.122, and 0.017 cm, respectively.

of $(\text{NH}_3)_y\text{Cs}_{0.4}\text{FeSe}$ were determined by the analysis to be $a = 3.8331(1)$ Å and $c = 16.217(1)$ Å (the crystallographic data are shown in the Supplemental Material),⁶ which shows that this sample contains three phases of $(\text{NH}_3)_y\text{Cs}_{0.4}\text{FeSe}$ (37%), β -FeSe (37%), and α -FeSe (26%). For this paper, we fully investigated the behavior of superconductivity in $(\text{NH}_3)_y\text{Cs}_{0.4}\text{FeSe}$ using this sample. Only a T_c of the $(\text{NH}_3)_y\text{Cs}_{0.4}\text{FeSe}$ phase is selectively extracted and discussed in this paper. Furthermore, the Rietveld refinement suggests that the exact chemical composition of $(\text{NH}_3)_y\text{Cs}_{0.4}\text{FeSe}$ is $(\text{NH}_3)_y\text{Cs}_{0.255(5)}\text{FeSe}$; i.e., the amount of Cs seems to be smaller than the nominal stoichiometry of Cs (0.4).

The a value [$3.8331(1)$ Å] for $(\text{NH}_3)_y\text{Cs}_{0.4}\text{FeSe}$ is a little larger than that determined for β -FeSe [$3.77179(4)$ Å] in this paper and the values reported previously for β -FeSe [$3.7747(1)$ or $3.7734(1)$ Å].⁷ However, the a [$3.8331(1)$ Å] is a little smaller than those for nonammoniated $\text{K}_{0.5}\text{FeSe}$ [$a = 3.9136(1)$ Å]¹ and $\text{Cs}_{0.4}\text{FeSe}$ [$a = 3.9601(2)$ Å].² The $c = 16.217(1)$ Å of $(\text{NH}_3)_y\text{Cs}_{0.4}\text{FeSe}$ is larger than those for β -FeSe [$c = 5.5234(1) \times 2 = 11.0468(2)$ Å or $c = 5.5228(1) \times 2 = 11.0456(2)$ Å in Ref. 7], nonammoniated $\text{K}_{0.5}\text{FeSe}$ [$c = 14.0367(7)$ Å],¹ and nonammoniated $\text{Cs}_{0.5}\text{FeSe}$ [$c = 15.2846(1)$ Å].² The larger c [$16.217(1)$ Å] in $(\text{NH}_3)_y\text{Cs}_{0.4}\text{FeSe}$ implies that NH_3 molecules are intercalated in the space between FeSe layers; i.e., both Cs atoms and NH_3 molecules are intercalated between FeSe layers. The predicted structure is shown in Fig. 2(b), where NH_3 molecules are not drawn because their exact locations are not determined in this

Rietveld refinement; a reliable location may not be determined from x-ray diffraction because of the small contribution of NH_3 (total number of electrons = 10) to x-ray scattering. Their exact location is determined only by neutron diffraction in $\text{Li}_{0.6(1)}(\text{ND}_2)_{0.2(1)}(\text{ND}_3)_{0.8(1)}\text{Fe}_2\text{Se}_2$.⁴ From the analogy with $\text{Li}_{0.6(1)}(\text{ND}_2)_{0.2(1)}(\text{ND}_3)_{0.8(1)}\text{Fe}_2\text{Se}_2$, NH_3 should coordinate with a Cs atom in $(\text{NH}_3)_y\text{Cs}_{0.4}\text{FeSe}$.

The $M/H-T$ plots in ZFC and FC modes for $(\text{NH}_3)_y\text{Cs}_{0.4}\text{FeSe}$ are shown in Fig. 2(c). The T_c^{onset} and T_c were determined to be 33.6 and 31.2 K, respectively [see the detail of T_c determination, Fig. 2(c) inset]. This T_c (31.2 K) is higher by 3.8 K than that of nonammoniated $\text{Cs}_{0.4}\text{FeSe}$ ($T_c = 27.4$ K).² The T_c increases with the increase in c from 15.2846(1) to 16.217(1) Å due to NH_3 insertion. The shielding fraction at 5 K was evaluated to be 31.2%, which is almost consistent with the fraction of $(\text{NH}_3)_y\text{Cs}_{0.4}\text{FeSe}$ determined from x-ray diffraction. The $M-H$ curve of $(\text{NH}_3)_y\text{Cs}_{0.4}\text{FeSe}$ is shown in the Supplemental Material.⁶ The lower critical field H_{c1} was evaluated to be 30 Oe (see the Supplemental Material).⁶ The resistivity ρ is plotted in Fig. 2(d) as a function of T ; ρ was evaluated from the measured R , channel length L , channel width W , and thickness d of the pellet sample [Fig. 2(d)]. The T_c^{onset} can be evaluated to be 36 K from the $\rho-T$ plot [Fig. 2(d)], which is higher than that determined from the $M/H-T$ plot [Fig. 2(c)]. The origin of the observed higher T_c^{onset} is still unclear, and complete zero resistivity was not observed as in Na- and Ba-doped FeSe prepared by the liquid NH_3 method.³ A small peak in ρ around T_c^{onset} is seen in the $\rho-T$ plot [Fig. 2(d)], which is consistent with the $\rho-T$ plots reported for ammoniated $\text{Na}_{0.5}\text{FeSe}$ and $\text{Ba}_{0.4}\text{FeSe}$.³ These features indicate that the same type of material as metal-intercalated FeSe compounds prepared previously using the NH_3 method³ was synthesized in this paper.

Here, we discuss the nanometer-scale phase-separation (antiferromagnetic [AFM] order phase and superconductor phase) found in nonammoniated metal-intercalated FeSe samples.^{10,11} The small peak around T_c is not observed in the $\rho-T$ plot of nanometer-scale phase-separated samples.¹¹ Therefore, the small peak does not imply the presence of nanometer-scale phase-separation in $(\text{NH}_3)_y\text{Cs}_{0.4}\text{FeSe}$. However, a hump is observed at ~ 200 K in $\rho-T$ plot of $(\text{NH}_3)\text{Cs}_{0.4}\text{FeSe}$, in the same manner as nonammoniated $M_x\text{FeSe}$ samples.¹¹ The hump often disappears even in the nonammoniated samples containing both the superconducting phase and the AFM order phase, depending on sample preparation, i.e., on topological features of superconducting parts.¹¹ Therefore, the relationship between the hump and the nanometer-scale phase separation (presence of the AFM order phase) is still unclear. Because of study with a powder sample, we cannot comment on the presence of an AFM order phase in $(\text{NH}_3)_y\text{Cs}_{0.4}\text{FeSe}$ or a nanometer-scale phase separation. There are no other reports on the presence of an AFM order phase in $(\text{NH}_3)_yM_x\text{FeSe}$.

The pressure dependence of χ' of $(\text{NH}_3)_y\text{Cs}_{0.4}\text{FeSe}$ is plotted in Fig. 3(a). The T_c is determined to be 31.8 K from the $\chi'-T$ plot measured at ambient pressure. This value is almost consistent with that determined from $M/H-T$ and $\rho-T$ plots [Figs. 2(c) and 2(d)]. The T_c decreases with an increase in pressure P , as seen from Figs. 3(a) and 3(b). The T_c-P plot is shown in Fig. 3(b), where red circles indicate the T_c

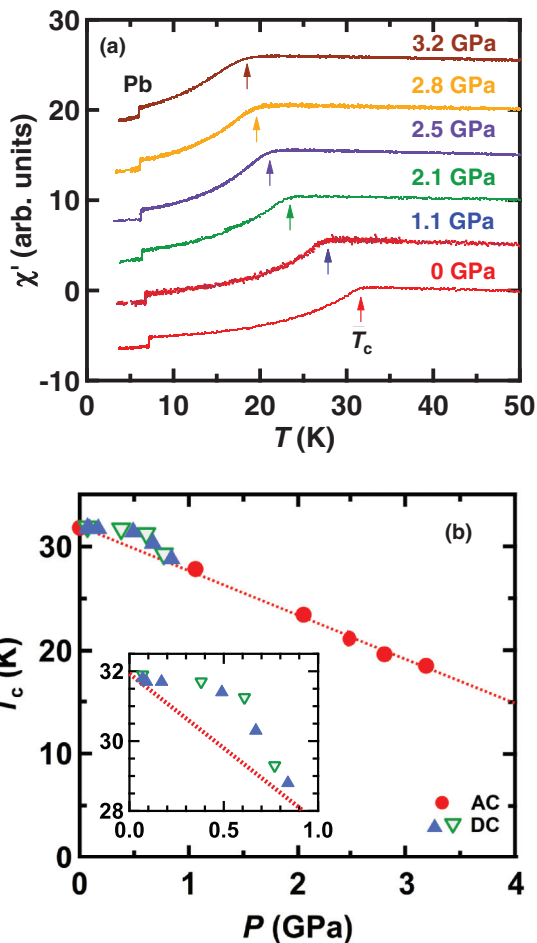


FIG. 3. (Color online) (a) $\chi'-T$ plots of $(\text{NH}_3)_y\text{Cs}_{0.4}\text{FeSe}$ sample under different pressures, and (b) pressure dependence of T_c . In (b), red circles indicate the T_c determined from $\chi'-T$ plot. Blue and green triangles indicate the T_c from $M/H-T$ plots measured in increasing and decreasing pressure, respectively. The line was fitted to the points, excluding the brief upward deviation enlarged in the inset, which shows data below 1 GPa in greater detail.

determined from the $\chi'-T$ plot [Fig. 3(a)]. The T_c decreases with an increase in pressure up to 3.2 GPa. The fitted line is drawn in Fig. 3(b), and the dT_c/dp is evaluated from it to be $-4.33(8)$ K GPa^{-1} . In order to precisely investigate the pressure dependence of T_c , the $M/H-T$ plot (not shown) was measured in the pressure range from ambient pressure to 0.83 GPa (low-pressure range). The T_c determined from $M/H-T$ is plotted with blue and green triangles in Fig. 3(b). As seen from Fig. 3(b), the triangle plots depart from the fitted line, showing a brief upward deviation. The deviation is more clearly shown in the inset of Fig. 3(b). The pressure dependence of T_c for nonammoniated Cs_xFeSe in the low-pressure range of 0.0–1.7 GPa showed a clear peak at 0.8 GPa, and the maximum T_c value was higher by ~ 1 K than that at ambient pressure.¹² The T_c-P plot for $(\text{NH}_3)_y\text{Cs}_{0.4}\text{FeSe}$ [Fig. 3(b) inset] does not show such a clear peak, but the brief upward deviation may be related to the T_c-P plot in nonammoniated Cs_xFeSe . Thus, we have investigated the pressure dependence of T_c in ammoniated metal-intercalated FeSe in the pressure range up to 3.2 GPa. We clarified that the T_c decreases monotonically

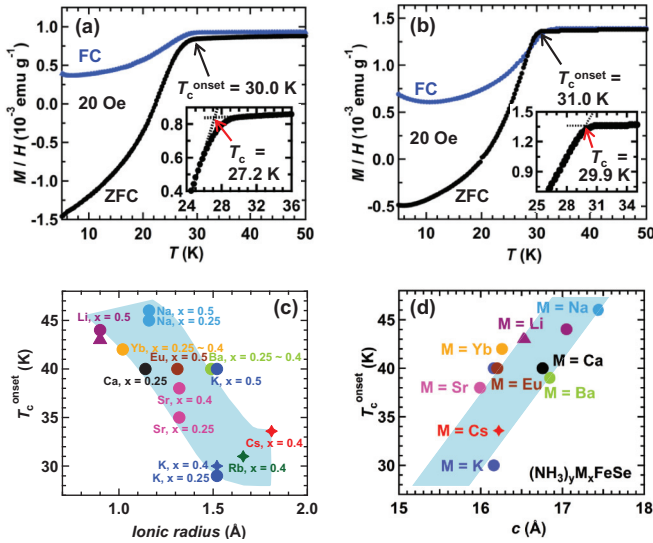


FIG. 4. (Color online) M/H - T plots of (a) $(NH_3)_yK_{0.4}FeSe$ and (b) $(NH_3)_yRb_{0.4}FeSe$ samples. Relationship (c) between T_c^{onset} and ionic radii of intercalated metal atoms and (d) between T_c^{onset} and c . In (c) and (d), the star-shaped symbols are plotted based on the data from this paper. Solid circle and triangle symbols are taken from Refs. 3 and 4, respectively.

in the high-pressure range but shows a brief elevation above linearity in the low-pressure range.

The M/H - T curves of $(NH_3)_yK_{0.4}FeSe$ and $(NH_3)_yRb_{0.4}FeSe$ are shown in Figs. 4(a) and 4(b), respectively. The T_c^{onset} and T_c are 30.0 and 27.2 K, respectively, for $(NH_3)_yK_{0.4}FeSe$, compared with 31.0 and 29.9 K, respectively, for $(NH_3)_yRb_{0.4}FeSe$. The 30.0-K T_c^{onset} of the $(NH_3)_yK_{0.4}FeSe$ prepared in this paper is the same as that of the $(NH_3)_yK_{0.4}FeSe$ prepared previously.³ Furthermore, the 30.0-K T_c^{onset} of $(NH_3)_yK_{0.4}FeSe$ is almost the same as the 31 K of nonammoniated $K_{0.4}FeSe$.¹ The $(NH_3)_yRb_{0.4}FeSe$ sample was prepared in this paper. The 31.0-K T_c^{onset} of $(NH_3)_yRb_{0.4}FeSe$ is almost the same as the 30.6 K of nonammoniated $Rb_{0.4}FeSe$.¹³ These results differ from those indicating that T_c increases by 3.8 K (from 27.4 to 31.2 K) in the case of ammoniated $Cs_{0.4}FeSe$. Since the expansion of c is confirmed (see the Supplemental Material),^{1,6,11} NH_3 molecules are intercalated in $(NH_3)_yK_{0.4}FeSe$ and $(NH_3)_yRb_{0.4}FeSe$. The small expansion of c in $(NH_3)_yK_{0.4}FeSe$ may explain the absence of any change in T_c , but the reason the T_c does not change in $(NH_3)_yRb_{0.4}FeSe$ is still unclear because of a significant expansion of c .

Figure 4(c) shows the plots of T_c^{onset} as a function of the ionic radii of the metal ions (M) in $(NH_3)_yM_{0.4}FeSe$. The T_c decreases rapidly with an increase in ionic radius. The T_c^{onset} for $(NH_3)_yLi_{0.5}FeSe$ is as high as 44 K,³ and the T_c^{onset} for $(NH_3)_yNa_xFeSe$ is 46 K,³ while the T_c^{onset} is the lowest (30 K) in $(NH_3)_yK_{0.4}FeSe$ and increases slightly to 33.6 K in $(NH_3)_yCs_{0.4}FeSe$. Thus, as evidenced in this paper, the insertion of K, Rb, and Cs, with larger ionic radii than the other metals, produces the lowest T_c s in the $(NH_3)_yM_{0.4}FeSe$ system. Furthermore, as seen from Fig. 4(d), the T_c clearly increases with an increase in c , suggesting that an increase in

two-dimensionality leads to an increase in T_c . Such a behavior is found in $HfNCl$ containing NH_3 and tetrahydrofuran molecules: When the plane spacing between $HfNCl$ layers increases, the T_c rapidly increases and saturates.¹⁴ In these materials, the maximum T_c is observed when the spacing between layers increases up to 15 Å because of an increase in nesting of the Fermi surface through a reduction of warping along the k_z direction.^{15,16} The plane spacing of 8.716 Å ($c/2$) in $(NH_3)_yNa_xFeSe$ produces the highest T_c at the present stage. Furthermore, the insertion of metal atoms with smaller ionic radii leads to both the expansion of c (or plane spacing) and an increase in T_c [Figs. 4(c) and 4(d)]. This implies a difference in the coordination structure of NH_3 with individual metal atoms or in the number of NH_3 molecules coordinating with each metal atom. In other words, the coordination of NH_3 molecules around Cs does not result in an expanded structure, while Li or Na may produce a larger coordination structure with NH_3 . These results are interesting in that coordination chemistry controls the T_c in this system. Thus, an increase in plane spacing between FeSe layers is important for the realization of high T_c in $(NH_3)_yM_xFeSe$, suggesting a clear correlation between an increase in two-dimensionality (or an increase in nesting of the Fermi surface) and superconductivity. This result may be interpreted as meaning that a spin-density wave (SDW) ground state with weak magnetic moments can stimulate the superconducting transition, as evidenced in $NaFe_{1-x}Co_xAs$ by scanning tunneling microscopy.¹⁷ Finally, we stress that the decrease in T_c with increasing pressure [Fig. 3(b)] is reasonable judging from the result that the T_c lowers with a decrease in c caused by an insertion of ions with larger ionic radii, as shown in Fig. 4(d), suggesting that the physical pressure effect in $(NH_3)_yCs_{0.4}FeSe$ can be uniformly understood with chemical pressure effect in $(NH_3)_yM_xFeSe$. This clearly shows that the scaling of T_c by FeSe plane spacing is meaningful. However, since the deviation from the straight line in the low-pressure range may not clearly be explained at the present stage, further study is indispensable for clarifying the mechanism.

In conclusion, we have prepared new ammoniated and metal-intercalated FeSe materials, and $(NH_3)_yCs_{0.4}FeSe$ shows a higher T_c than nonammoniated $Cs_{0.4}FeSe$. Furthermore, a clear correlation between T_c and plane spacing was observed, suggesting that an increase in nesting of the Fermi surface may produce higher T_c . In this paper, we did not discuss other scaling parameters, such as anion height or bonding angle found in $LaFeAsO$ compounds,^{18,19} but the scaling of T_c by FeSe plane spacing may be simpler and more understandable from physical point of view. Thus, the superconducting pairing in this system may also be caused by magnetic fluctuation in a weak SDW magnetic state, suggesting that this material is an unconventional superconductor. Consequently, this paper on new members in the $(NH_3)_yM_xFeSe$ family provided understanding for metal-intercalated FeSe materials.

Y.K. greatly appreciates S. Clarke of Oxford University for his suggestion. This paper is partly supported by Grants-in-Aid (No. 22244045 and No. 24654105) of Japan's Ministry of Education, Culture, Sports, Science and Technology and by the Light Element Molecular Superconductivity project (Japan

Science and Technology Agency–European Union Superconductor Project). The x-ray diffractions with synchrotron

radiation were done under the proposals of SPring-8 (Proposals No. 2011A1938 and No. 2011B1496).

*Present address: Research Laboratory for Surface Science, Okayama University, Okayama 700-8530, Japan, e-mail: kubozone@cc.okayama-u.ac.jp

- ¹J. G. Guo, S. F. Jin, G. Wang, S. C. Wang, K. X. Zhu, T. T. Zhou, M. He, and X. L. Chen, *Phys. Rev. B* **82**, 180520(R) (2010).
- ²A. Krzton-Maziopa, Z. Shermadini, E. Pomjakushina, V. Pomjakushin, M. Bendele, A. Amato, R. Khasanov, H. Luetkens, and K. Conder, *J. Phys. Condens. Matter* **23**, 052203 (2011).
- ³T. P. Ying, X. L. Chen, G. Wang, S. F. Jin, T. T. Zhou, X. F. Lai, H. Zhang, and W. Y. Wang, *Sci. Rep.* **2**, 426 (2012).
- ⁴M. Burrard-Lucas, D. G. Free, S. J. Sedlmaier, J. D. Wright, S. J. Cassidy, Y. Hara, A. J. Corkett, T. Lancaster, P. J. Baker, S. J. Blundell, and S. J. Clarke, *Nat. Mater.* **12**, 15 (2013).
- ⁵T. P. Ying, X. L. Chen, G. Wang, S. F. Jin, X. F. Lai, T. T. Zhou, H. Zhang, S. J. Shen, and W. Y. Wang, *J. Am. Chem. Soc.* **135**, 2951 (2013).
- ⁶See Supplemental Material at <http://link.aps.org/supplemental/10.1103/PhysRevB.88.094521> for sample preparations and crystallographic data of FeSe and $(\text{NH}_3)_y\text{M}_x\text{FeSe}$, M - H curve of $(\text{NH}_3)_y\text{Cs}_{0.4}\text{FeSe}$, and the lattice constants of $(\text{NH}_3)_y\text{K}_{0.4}\text{FeSe}$ and $(\text{NH}_3)_y\text{Rb}_{0.4}\text{FeSe}$.
- ⁷T. M. McQueen, Q. Huang, V. Ksenofontov, C. Felser, Q. Xu, H. Zandbergen, Y. S. Hor, J. Allred, A. J. Williams, D. Qu, J. Checkelsky, N. P. Ong, and R. J. Cava, *Phys. Rev. B* **79**, 014522 (2009).
- ⁸M. Takata, *Acta Crystallogr. Sect. A* **64**, 232 (2008).
- ⁹T. C. Kobayashi, H. Hidaka, H. Kotegawa, K. Fujiwara, and M. I. Eremets, *Rev. Sci. Instrum.* **78**, 023909 (2007).
- ¹⁰Y. Liu, Q. Xing, K. W. Dennis, R. W. McCallum, and T. A. Lograsso, *Phys. Rev. B* **86**, 144507 (2012).
- ¹¹X. X. Ding, D. L. Fang, Z. Y. Wang, H. Yang, J. Z. Liu, Q. Deng, G. B. Ma, C. Meng, Y. H. Hu, and H.-H. Wen, *Nat. Comm.* **4**, 1897 (2013).
- ¹²J. J. Ying, X. F. Wang, X. G. Luo, Z. Y. Li, Y. J. Yan, M. Zhang, A. F. Wang, P. Cheng, G. J. Ye, Z. J. Xiang, R. H. Liu, and X. H. Chen, *New J. Phys.* **13**, 033008 (2011).
- ¹³A. F. Wang, J. J. Ying, Y. J. Yan, R. H. Liu, X. G. Luo, Z. Y. Li, X. F. Wang, M. Zhang, G. J. Ye, P. Cheng, Z. J. Xiang, and X. H. Chen, *Phys. Rev. B* **83**, 060512(R) (2011).
- ¹⁴G. J. Ye, J. J. Ying, Y. J. Yan, X. G. Luo, P. Cheng, Z. J. Xiang, A. F. Wang, and X. H. Chen, *Phys. Rev. B* **86**, 134501 (2012).
- ¹⁵T. Takano, T. Kishiume, Y. Taguchi, and Y. Iwasa, *Phys. Rev. Lett.* **100**, 247005 (2008).
- ¹⁶S. Yamanaka, *J. Mater. Chem.* **20**, 2922 (2010).
- ¹⁷P. Cai, X. D. Zhou, W. Ruan, A. F. Wang, X. H. Chen, D.-H. Lee, and Y. Y. Wang, *Nat. Comm.* **4**, 1596 (2013).
- ¹⁸C.-H. Lee, A. Iyo, H. Eisaki, H. Kito, M. T. Fernandez-Diaz, T. Ito, K. Kihou, H. Matsuhata, M. Braden, and K. Yamada, *J. Phys. Soc. Jpn.* **77**, 083704 (2008).
- ¹⁹Y. Mizuguchi and Y. Takano, *J. Phys. Soc. Jpn.* **79**, 102001 (2010).